



Understanding forest biomass and net primary productivity in Himalayan ecosystem using geospatial approach

Srishti Gwal¹ · Sarnam Singh^{2,3} · Stutee Gupta⁴ · Shikha Anand⁴

Received: 25 March 2020 / Accepted: 4 June 2020 / Published online: 18 June 2020
© Springer Nature Switzerland AG 2020

Abstract

Forest operates as sink–source of the atmospheric CO₂; hence, they form the integral part of terrestrial global carbon cycle. Biomass and primary productivity are the crucial dynamic biophysical parameters for understanding the ecosystem functioning in any forested landscape. The present study was performed in Aglar watershed situated in outer Indian Himalayan range. We performed geospatial modeling of plot-level field data on forest above ground biomass (AGB) by correlating it with textural, spectral and linearly transformed variables retrieved from Landsat 8 OLI data using of random forest (RF) machine learning algorithm. We also applied recursive feature elimination function (RFE) to obtain the variables contributing most in AGB prediction. A combination of 24 among 96 variables was identified as the most effective variables. Ground-based AGB varied from 62.54 to 470.98 Mg ha⁻¹, whereas RF-modeled AGB ranged from 48.5 to 407.73 Mg ha⁻¹. Results indicated that RFE selected variables were able to predict AGB with R^2 of 0.84, RMSE of 42.03 Mg ha⁻¹, MAE of 34.68 and %RMSE of 19.49 Mg ha⁻¹ which was accepted considering the terrain complexity. Light use efficiency approach was used to model monthly NPP using Landsat 8 OLI data. The results indicated that *Quercus* mixed forest had highest carbon assimilation (95,148,073.9 gC) followed by *Pinus roxburghii* (1,863,187.7 gC), *Cedrus deodara* (5,752,954.1 gC) and mixed forest (2,634,737.1 gC). The seasonal pattern of NPP indicated that its strike peaked in October, whereas December and January were the lean months, suggesting that NPP is governed by climatic factors, viz. PAR, precipitation and temperature. Such watershed-level study in complex Himalayan terrain would help to understand complex biogeochemical processes in basins and ecosystem services provided by the forests.

Keywords Forest AGB · NPP · Random forest · LUE · Aglar watershed · Western Himalaya · Geospatial modeling

Introduction

Forest biomass and net primary productivity (NPP) form an integral part of the global terrestrial carbon cycle by operating as sink–source of atmospheric CO₂ (Dixon et al. 1994; Pan et al. 2011). These are crucial biophysical parameters for understanding ecosystem functioning in any forested landscape. Forest biomass and NPP are known to have causal correlation (Cramer et al. 1999). However, mere observation of increase in carbon storage of a forest vegetation would be insufficient to acknowledge the increase in productivity (Keeling and Phillips 2007). Thus, site-specific factors, viz. temperature, moisture and nutrient availability influencing the process of carbon assimilation, must be taken into consideration for productivity assessment (Lieth 1975; Melillo et al. 1993; Laurance et al. 1999; Knapp and Smith 2001; Malhi et al. 2004; Raich et al. 2006).

✉ Srishti Gwal
sristigwal01@gmail.com

Sarnam Singh
sarnam.singh@gmail.com

Stutee Gupta
stutee_g@nrsc.gov.in

Shikha Anand
shikha.anand911@gmail.com

¹ Forestry and Ecology Department, Indian Institute of Remote Sensing, Indian Space Research Organisation (ISRO), Dehradun, Uttarakhand 248 001, India

² Indian Institute of Remote Sensing, Indian Space Research Organisation, Dehradun, Uttarakhand 248 001, India

³ School of Ecology and Environment Studies, Nalanda University, Rajgir, Nalanda, Bihar 803116, India

⁴ National Remote Sensing Centre, Indian Space Research Organisation, Hyderabad, Telangana 500037, India

Forest biomass represents the potential amount of living or dead organic matter that gets added to the biosphere, whereas NPP signifies the rate at which net assimilation of organic carbon by green vegetation occurs over a period. Thus, their quantification becomes imperative for discerning the energy flow exchanges and nutrients fluxes in a terrestrial ecosystem, more importantly in a complex mountainous terrain (Chave et al. 2008; Shirima et al. 2015). Two most widely followed approaches for estimation of forest AGB are: ground-based and remote sensing (RS)-based methods combined with field data (Roy and Ravan 1996; Kale et al. 2002; Tiwari et al. 2005; Kumar et al. 2011; Singh et al. 2012; Devagiri et al. 2013; Salunkhe et al. 2016). Certainly, ground-based methods furnish precise information but are time-labor intensive and destructive to semi-destructive in nature (de Gier 2003). They also fail to capture the overall spatiotemporal micro-climatic variability when practiced in rugged mountainous terrain on large scale. An alternate to prior approach is to use satellite data based on RS technique, since it is amenable to produce synoptic and time-series coverage of an area (Kale et al. 2002; Patenaude et al. 2005; Rosillo-Calle 2007; Ravindranath and Ostwald 2008). Maisongrande et al. (1995), Nelson et al. (2000), Lu et al. (2004) and Lu (2005) have utilized satellite data-derived variables as predictor variables for geospatial modeling of forest above ground biomass (AGB) by applying either empirical or biophysical process-based models (Kale et al. 2002; Gasparri et al. 2010; Manna et al. 2014). However, selection of the method is usually based on the availability of the input parameters, micro-climatic and topographic conditions of the region. In Indian scenario, AGB assessments were done by developing regression equations between crown cover and stand biomass using satellite data in different eco-regions in western Himalaya (Tiwari and Singh 1984; Tiwari 1994; Tiwari et al. 2005). Kale et al. (2002, 2005) and Kumar et al. (2011) applied similar approach for AGB assessment in tropical forest ecosystems of Central India and Shivalik Himalaya. Singh et al. (2012) performed spatial up-scaling of AGB using multi-season NDVI images of MODIS satellite data in temperate forests of Jammu & Kashmir Himalaya. Upp Gupta et al. (2015) used very high-resolution data of Cartosat-1 and Quick Bird to assess AGB of forest plantations. Though majority of studies have used few VIs for spectral modeling of AGB many authors have reported saturation of VIs at higher biomass values (Steininger 2000; Kasischke et al. 2014). Hence, attempts are being made to develop suitable regression models world over (Lu 2006; Mutanga et al. 2012). Random forest (RF) algorithm is an ensemble technique that exploits bagging and boosting to perform classification and regression analyses (Breiman 2001). With a modest fine-tuning of parameters, the RF algorithm produces

outcomes with high accuracy at high computational speed (Gislason et al. 2006; Lawrence et al. 2006; Meacham et al. 2016; Liu et al. 2017; Safari et al. 2017; Le et al. 2018; Pandit et al. 2018a; Teluguntla et al. 2018). The algorithm is also capable of predicting important independent variables w.r.t. dependent variable by using recursive feature elimination function (RFE) (Guyon and Elisseeff 2003; Ismail and Mutanga 2010; Belgiu and Drăgu 2016; Dang et al. 2019).

NPP is recognized as key indicator for assessing ecosystem pattern, processes and its overall health. The increased availability of RS data has excelled the count of models simulating dynamics of NPP over a time. Cramer et al. (1999) and Ruimy et al. (1999) have reviewed productivity models in two groups, viz. production efficiency model (PEMs) and canopy production model (CPMs). The diagnostic PEMs rely on the concept of light use efficiency (LUE)—‘the efficiency with which light energy is used by the vegetation to sequester carbon’ (Monteith 1972; Kumar and Monteith 1981). A few examples of PEMs coupled with RS data are Global-PEM (Prince and Goward 1995), Carnegie–Ames–Stanford Approach ‘CASA’ (Potter et al. 1993), Carbon Fixation (C-Fix), etc. The prognostic CPMs such as Global Biome Model (Haxeltine and Prentice 1996), Carbon Assimilation the Biosphere (Warnant et al. 1994), HYBRID (Friend and Cox 1995), etc., follow the principles of major biophysical processes, viz. photosynthesis, respiration and allocation of assimilates. Modeling of NPP through CPMs requires various field-derived eco-physiological inputs, whereas LUE model utilizes fraction of absorbed photosynthetically active radiation (fAPAR) and LUE (ϵ_{\max}). Roy and Jain (1998), Kale et al. (2002) and Kale and Roy (2012) estimated NPP using PEMs in tropical deciduous forests of central India. Chhabra and Dadhwal (2004), Nayak et al. (2010), Chitale et al. (2012) and Nayak et al. (2013, 2015) used C-Fix and CASA models to estimate monthly NPP over the Indian subcontinent. Singh et al. (2011) studied the inter-annual variability in NPP using Global-PEM model. Tripathi et al. (2018) and Behera et al. (2019) estimated monthly NPP in the forests of Northern India using CASA and Biome BGC models. The process of estimation of NPP has transformed now for monitoring of in situ carbon fluxes (Chhabra and Dadhwal 2004; Goroshi et al. 2014; Dadhwal 2012; Deb Burman et al. 2017). However, due to unavailability of in situ data, only limited number of studies related to biomass and carbon dynamics are reported from remote interiors of Indian Himalaya Region (IHR). Despite holding 39.33% forest cover of the total geographical area, the forest ecosystems of IHR are insufficiently studied in terms of NPP specifically at basin and watershed scales. Under such scenario, the present study is an attempt (a) to estimate forest AGB using RF algorithm and (b) to assess spatiotemporal

variation in forest NPP using LUE approach in a Himalayan watershed.

Materials and methods

Study area

Aglar watershed lies from 30° 27' 4" to 30° 38' 5" N and 77° 56' 15" to 78° 18' 45" E in Tehri-Garhwal district of Uttarakhand, India (Fig. 1a). The watershed covers an area of ~307.28 km² with altitudinal variation of 690–3015 amsl,

representing tropical to humid temperate biomes. The highest rainfall is recorded in the months of June to September and the lowest in December with an annual average of > 2000 mm (IMD 2015). The altitudinal gradient and climatic conditions favor a variety of vegetation formations. The dominant vegetation types are gregarious formations of Himalayan Moist Temperate forest of *Quercus leucotrichophora*, *Quercus floribanda* and *Cedrus deodara*, Himalayan subtropical Pine forest (*Pinus roxburghii*) and tropical mixed miscellaneous forest with dominant species like *Grewia optiva*, *Terminalia chebula*, *Bauhinia variegata*, etc. However, the lower heights of southern aspect are mostly

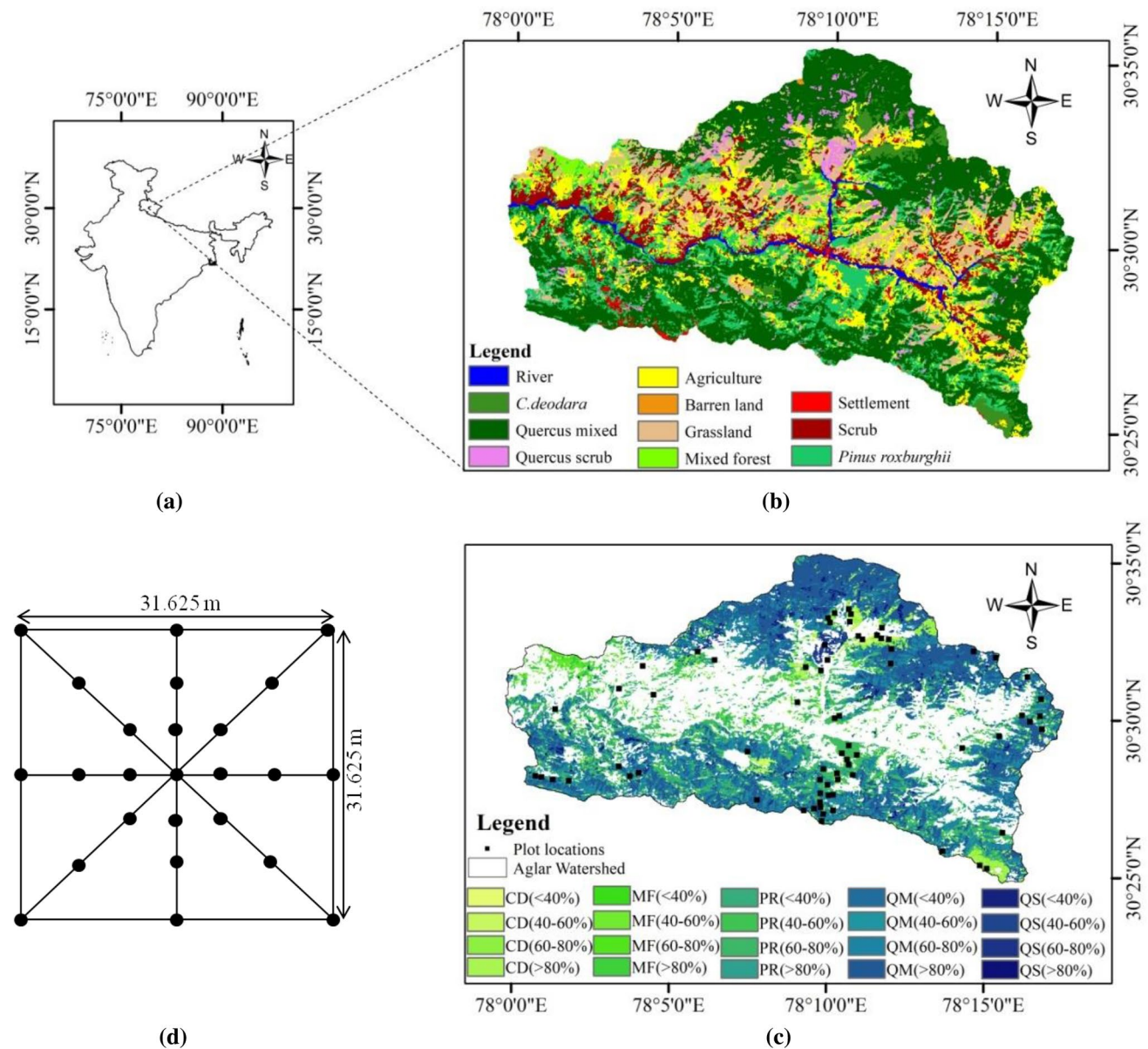


Fig. 1 a Location map of Uttarakhand, India b LULC and c homogeneity map of Aglar watershed (CD = *Cedrus deodara*, MF = Mixed forest, PR = *Pinus roxburghii*, QM = *Quercus mixed*, QS = *Quercus scrub*), and d LAI sampling points per 0.1 ha plot

dominated by subtropical scrub, grasslands interspersed with agricultural fields (Fig. 1b).

Satellite data and preprocessing

The ortho-rectified images of Landsat-8 OLI with 30 m spatial resolution were used for mapping of forest cover type, forest density and modeling of forest AGB and NPP (illustrated in Fig. 2). The cloud-free data for each month of the year 2015 were downloaded from <https://earthexplorer.usgs.gov> except for July and August due to thick cloud cover because of prevailing monsoon season. For modeling of forest AGB, 17 April 2015 image was chosen when forest vegetation has distinct foliage cover. The entire dataset was atmospherically corrected using which VIs, textural components and linearly transformed images were generated (Table 1).

Ground data collection

A stratified random sampling approach based on homogeneity map was followed to capture the variability of forest types, forest density and terrain conditions (Fig. 1c). The forest cover type and density cover maps were prepared from

dry and growing season Landsat-8 OLI images. To determine sample size, a few samples were laid initially to ascertain the variance and range of bole diameter, tree height and biomass in each stratum. The sample size was determined using Chako’s formula (1965) (Eq. 1)

$$N = t^2 \times (\text{Coefficient of variation})^2 / (\% \text{ Standard error})^2 \tag{1}$$

where N is sample size and t is value of t test at 95% confidence level.

Resultantly, considering probability proportion to its size, 71 sample plots of 0.1 ha were distributed across the different strata. Relevé size was based on earlier studies of Forest Department. Ground inventory on species, tree diameter at breast height (i.e., 1.37 m), tree height, canopy closure, number of storys, soil characteristics, pH, etc., were noted. The monthly leaf area index (LAI) observations were collected from 14 representative plots with the help of a well-calibrated AccuPARLP-80 Ceptometer. The LAI measurements were taken by traversing the area in all directions during early or late hours of the day or under sky cast conditions to avoid speckle effect of direct sunlight (Fig. 1d).

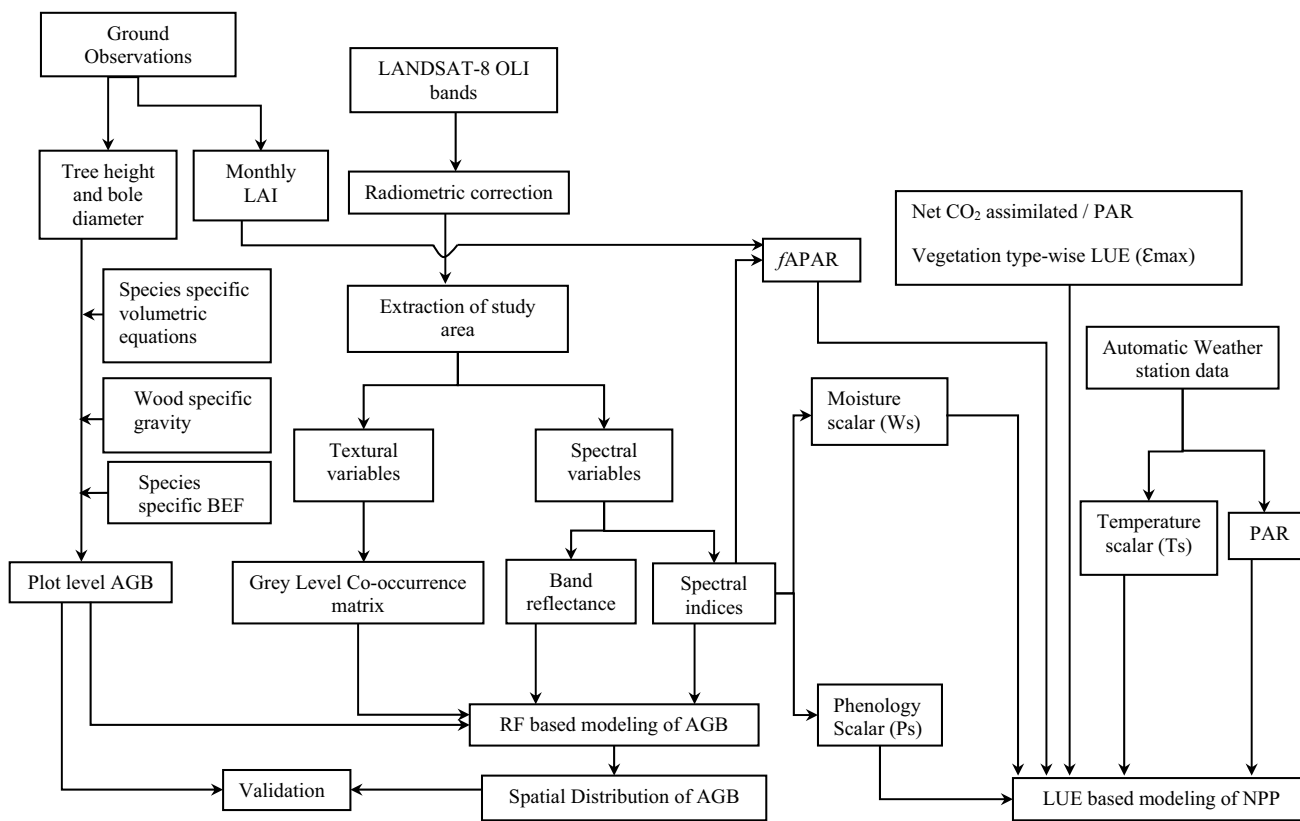


Fig. 2 Methodology paradigm for assessing geospatial pattern of AGB and NPP

Table 1 List of predictor variables computed from Landsat 8 OLI image for AGB modeling

S. no.	Variables	Full Name	Formula	References
1.	Spectral bands (6)	Band2	Blue	Zanter (2016)
		Band3	Green	
		Band4	Red	
		Band5	NIR	
		Band6	SWIR1	
		Band7	SWIR2	
		2.	Simple ratios (7)	
Red by Green	Red/Green			Gamon and Surfus (1999)
SWIR1 by SWIR2	SWIR1/SWIR2			Singh et al. (2014)
NIR by Green	NIR/Green			Kimura et al. (2004)
SWIR2 by Red	SWIR2/Red			Lu et al. (2004)
NIR by SWIR2	NIR/SWIR2			Kimura et al. (2004)
NIR by Red	NIR/Red			Birth and McVey (1968)
3.	Complex ratios (30)	Atmospherically Resistant Vegetation Index (ARVI)	$NIR - RB/NIR + RB$ where $RB = \gamma(Red - Blue)$ and $\gamma = 1$ when aerosol model is unavailable.	Kaufman and Tanre (1992)
		Differenced Vegetation Index (DVI)	$NIR - Red$	Tucker (1979)
		Enhanced Vegetation Index (EVI)	$2.5 \times (NIR - Red) / (NIR + 6 \times Red - 7.5 \times Blue) + 1$	Bannari et al. (1995)
		Green Atmospherically Resistant Vegetation Index (GARI)	$NIR - (Green - (Blue - Red)) / NIR - (Green + (Blue - Red))$	Gitelson et al. (1996)
		Green Difference Vegetation Index (GDVI)	$NIR - Green$	Sripada et al. (2006)
		Global Environment Monitoring Index (GEMI)	$\eta(1 - 0.25\eta) - (Red - 0.125) / (1 - Red)$	Myneni et al. (1995)
		Green Normalized Vegetation Index (GNDVI)	$(NIR - Green) / (NIR + Green)$	Gitelson et al. (1996)
		InfraRed Percentage Vegetation Index (IPVI)	$(NIR) / (NIR + Red)$	Crippen (1990)
		Modified Soil-Adjusted Vegetation Index2 (MSAVI2)	$(1/2) \times (2NIR + 1) - (\sqrt{(2 \times NIR + 1)^2 - 8 \times (NIR - Red)})$	Qi et al. (1994)
		Moisture Stress Index (MSI)	$SWIR1/NIR$	Raymond Hunt et al. (1987)
		Enhanced Moisture Stress Index (EMSI)	$SWIR2/NIR$	Vogelmann and Rock (1985)
		Modified Simple Ratio (MSR)	$(NIR/Red) - 1/\sqrt{(NIR/Red) + 1}$	Chen (1996)
		Modified Normalized Difference Vegetation Index (mNDVI)	$NIR - SWIR2 / NIR + SWIR2$	Jurgens (1997)
		Modified Nonlinear Vegetation Index (MNLI)	$(1 + L)(NIR^2 - Red) / (NIR^2 + Red + L)$	Gong et al. (2003)
		Normalized NIR (NNIR)	$NIR / (NIR + Red + Green)$	Majasalmi and Rautiainen (2016)
		Normalized Difference InfraRed Index (NDII)	$NIR - SWIR1 / NIR + SWIR1$	Hardisky et al. (1983)
		Nonlinear Vegetation Index (NLI)	$(NIR)^2 - Red / (NIR)^2 + Red$	Goel and Qin (1994)
		Normalized Difference Water Index (NDWI)	$(Green - NIR) / (Green + NIR)$	Gao (1996)
		Normalized Difference Vegetation Index (NDVI)	$NIR - Red / NIR + Red$	Rouse et al. (1973)
		Normalized Green (Norm G)	$Green / (NIR + Red + Green)$	Kender (1976)
Optimized Soil-Adjusted Vegetation Index (OSAVI)	$(NIR - Red) / (NIR + Red + 0.16)$	Rondeaux et al. (1996)		
Renormalized Difference Vegetation Index (RDVI)	$(NIR - Red) / \sqrt{(NIR - Red)}$	Roujean and Breon (1995)		

Table 1 (continued)

S. no.	Variables	Full Name	Formula	References
		Normalized Red (Norm R)	$\text{Red}/(\text{NIR} + \text{Red} + \text{Green})$	Kender (1976)
		Soil-Adjusted and Atmospherically Resistant Vegetation Index (SARVI)	$(1 + L) \times (\text{NIR} - \text{Red}) / (\text{NIR} + \text{Red} + L)$	Kaufman and Tanre (1992)
		Soil-Adjusted Vegetation Index (SAVI)	$(1 + L)((\text{NIR} - \text{Red}) / (\text{NIR} + \text{Red} + L))$	Huete (1988)
		Specific Leaf Vegetation Index (SLAVI)	$\text{NIR}/\text{Red} + \text{SWIR}$	Lymburner et al. (2000)
		Transformed Vegetation Difference Index (TDVI)	$1.5 \times ((\text{NIR} - \text{Red}) / (\text{sqrt}(\text{NIR}^2 + \text{Red} + 0.5)))$	Bannari et al. (2002)
		Wide Dynamic Range Vegetation Index (WDRVI)	$((0.1 \times \text{NIR}) - \text{Red}) / ((0.1 \times \text{NIR}) + \text{Red})$	Gitelson (2004)
		Transformed Vegetation Index (TVI)	$\text{Sqrt}(\text{Red} - \text{Green}) / (\text{Red} + \text{Green}) + 0.5$	Rouse et al. (1973)
		Visible Atmospherically Resistant Index (VARI)	$(\text{Green} - \text{Red}) / (\text{Green} + \text{Red} - \text{Blue})$	Gitelson et al. (2002)
4.	Linear transformation (5)	Tasseled cap angle (TCA)	$\arctan(\text{TCG}/\text{TCB})$	Kauth (1976)
		Tasseled cap brightness (TCB)	$\text{Blue} \times 0.3029 + \text{Green} \times 0.2786 + \text{Red} \times 0.4733 + \text{NIR} \times 0.5599 + \text{SWIR1} \times 0.508 + \text{SWIR2} \times 0.1872$	
		Tasseled cap distance (TCD)	$\sqrt{(\text{TCB})^2 + (\text{TCG})^2}$	
		Tasseled cap greenness (TCG)	$\text{Blue} \times (-0.2941) + \text{Green} \times (-0.243) + \text{Red} \times (-0.5424) + \text{NIR} \times (0.7276) + \text{SWIR1} \times (0.0713) + \text{SWIR2} \times (-0.1608)$	
		Tasseled cap wetness (TCW)	$\text{Blue} \times (0.1511) + \text{Green} \times (0.1973) + \text{Red} \times (0.3283) + \text{NIR} \times (0.3407) + \text{SWIR1} \times (-0.7117) + \text{SWIR2} \times (-0.4559)$	
5.	Texture (48)	Mean (b1)	$3 \times 3, 5 \times 5, 7 \times 7, 9 \times 9$ for band 2,	Haralick (1979)
		Variance (b2)	$3, 4, 5, 6$ and 7	
		Homogeneity (b3)		
		Contrast (b4)		
		Dissimilarity (b5)		
		Entropy (b6)		
		2nd Moment (b7)		
		Correlation (b8)		

Estimation of forest AGB

The species-specific volumetric equations developed by FSI (1996) were applied to get volume of individual trees. Tree volume was multiplied with wood-specific gravity (FRI 2002) to obtain bole biomass. Biomass expansion factor was used to obtain total tree biomass (Haripriya 2002). The individual tree biomass was summed up to obtain plot-level biomass and then factorized to get pixel-level biomass. For geospatial modeling of AGB, RF algorithm from RandomForest package was applied in R-environment. The algorithm combines large sets of decision

trees formed by selecting sets of variables to improve classification and regression analysis. We used recursive feature elimination function (RFE) to find out important independent variables w.r.t. dependent variable. RFE was performed over 96 variables consisting of 6 spectral bands, 5 linear transformed images, 7 simple ratios, 30 complex ratios and 48 textural (5×5) variables. Effective set of 24 variables were identified on the basis lowest RMSEC value marked as red circle in Fig. 3. For modeling, 2/3 rd of the samples ($n = 53$), also called in-bag samples, were utilized for training the algorithm, and 1/3 rd of the samples, i.e., out-of-bag ‘OOB’ samples ($n = 18$), were

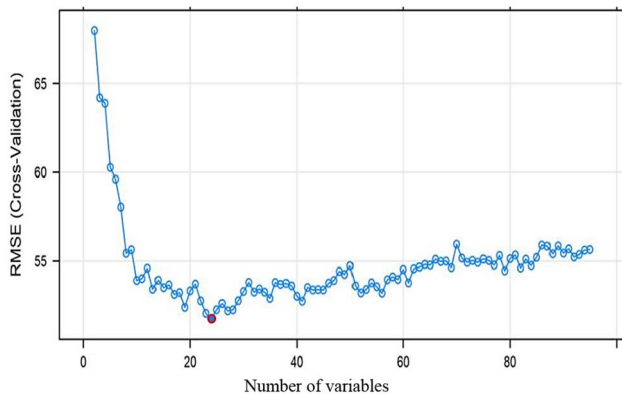


Fig. 3 RFE-based selection of optimum variables

used for cross-validation to determine the model error (or OOB error). Major parameters required for proper optimization of RF were: ‘ntree,’ i.e., total number of regression trees grown from bootstrap sample of the observations; ‘mtry’ was the number of predictor variables examined on each node, and ‘node-size’ was the smallest size of the end nodes of the trees grown. After multiple iterations, the optimum ‘ntree’ selected was 500 at ‘mtry’ = 8 as it resulted into the small OOB error.

Estimation of NPP

The integration of LUE and process-based model was identified as an efficient approach to model NPP using RS data (Kale et al. 2002; Lu et al. 2010). NPP is predominantly affected by ϵ^* (realized LUE) and absorbed photosynthetic active radiation (APAR) (Monteith 1972) and were obtained from Eqs. 2 and 3, respectively.

$$NPP = \epsilon^* \times APAR \tag{2}$$

$$APAR = fAPAR \times PAR \tag{3}$$

where PAR stands for photosynthetic active radiation in visible range (400–700 nm) calculated as 45–50% (Potter et al. 2003) of the shortwave radiation, and fAPAR is the fraction of absorbed radiation and was calculated using Eq. 4 (Ruimy et al. 1999).

$$fAPAR = 0.95 \times (1 - e^{-k \times LAI}) \tag{4}$$

k in Eq. 4 is the light extinction coefficient and was set as 0.5 (Jarvis and Leverenz 1983), and LAI is the leaf area index modeled by regressing field-observed monthly/seasonal LAI with corresponding NDVI.

The complex interactions between vegetation structure, soil moisture, climatic factors and solar radiation affect maximum LUE (ϵ_{max}) to govern the spatiotemporal

variations of forest productivity (Kale et al. 2002; Nemani et al. 2003). Therefore, integration of temperature (T_s) and moisture scalar (W_s) was important in order to get ϵ^* of a species in different forest ecosystems (Eq. 5).

$$\epsilon^* = \epsilon_{max} \times T_s \times W_s \times P_s \tag{5}$$

For the present study, ϵ_{max} value for different forest types was obtained from (Nayak et al. 2010). Terrestrial ecosystem model-based T_s (Raich 1991) and LSWI-based W_s (Xiao et al. 2005) were obtained from Eqs. 6 and 7.

$$T_s = \frac{(T - T_{min})(T - T_{max})}{(T - T_{min})(T - T_{max}) - (T - T_{opt})^2} \tag{6}$$

where T_{min} , T_{max} , T_{opt} and T are minimum, maximum, optimum and average air temperatures (in °C), respectively. We used T_{min} and T_{max} (2.68 °C and 23 °C, respectively) as recorded by Automatic Weather Station (AWS) installed in the area. T_{opt} for photosynthesis in temperate evergreen forest ranges from 10 to 25 °C. It was set 21 °C and was used obtained from Cunningham and Read (2002).

$$W_s = \frac{1 + LSWI}{1 + LSWI_{max}} \tag{7}$$

where $LSWI_{max}$ stands for maximum value of LSWI for each pixel in the growing period.

To account for leaf developmental stage, phenology scalar (P_s) was obtained from Xiao et al. (2004) (Eq. 8).

$$P_s = \frac{1 + LSWI}{2} \tag{8}$$

Similar approach was adopted by Huang et al. (2010) to model NPP in mountainous forest of Guangdong Province, China.

Results and discussion

Estimation of AGB

A total 3317 trees were measured for bole diameter (dbh) and tree height. The tree density (per 0.1 ha) ranged from 23 to 147 in *Quercus* (Oak) mixed forest, 17 to 73 in *Cedrus deodara* (Deodar) forest, 12 to 56 in *Pinus roxburghii* (Pine) forest and 27 to 82 in mixed miscellaneous forest. The diameter in *Quercus* forest ranged from 12.61 to 40.63 cm (± 6.45 SD), for *Cedrus deodara* forest from 27.47 to 58.64 cm (± 10.71 SD), for *Pinus roxburghii* forest from 17.27 to 56.85 cm (± 12.48 SD) and for mixed forest it was from 19.78 to 21.26 cm (± 0.52 SD).

AGB based on primary data ranged from 325.86 to 470.98 Mg ha⁻¹ (± 37.44 SD) in *Cedrus*

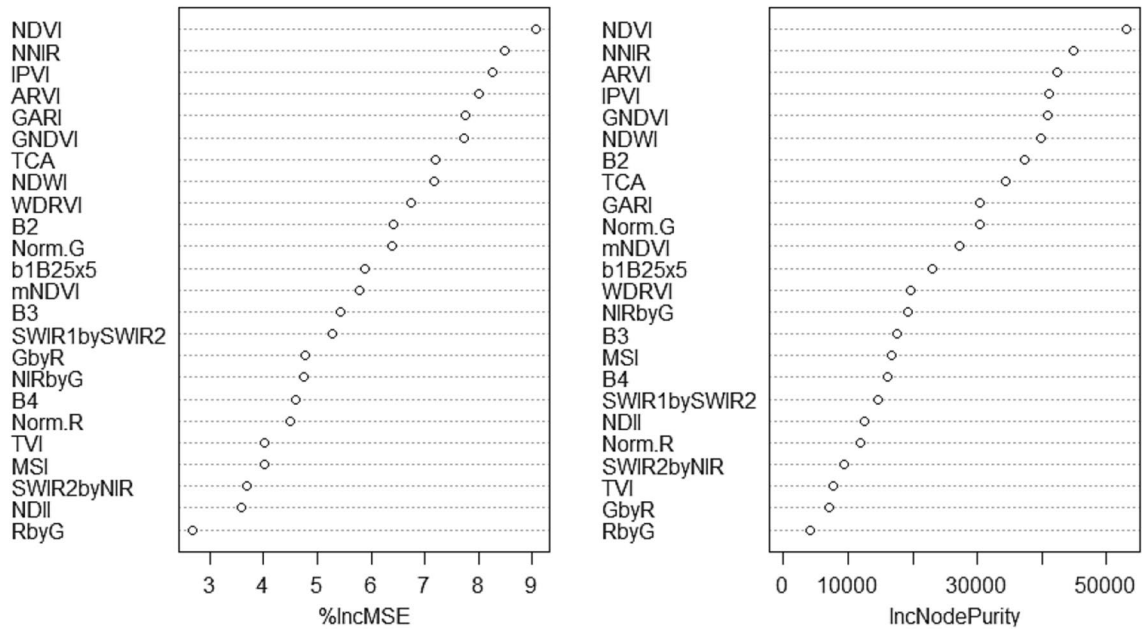


Fig. 4 Relative importance of variables selected by RFE (refer Table 1 for details)

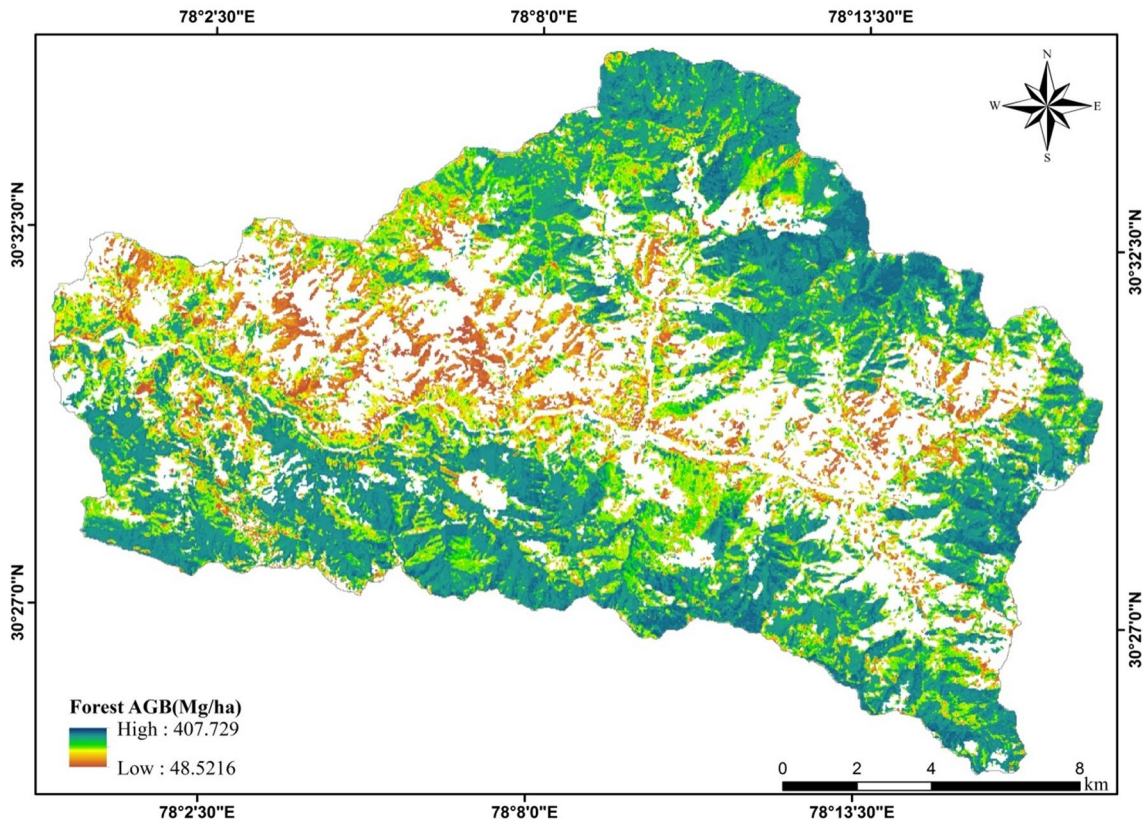


Fig. 5 Spatial distribution of AGB in Aglar watershed

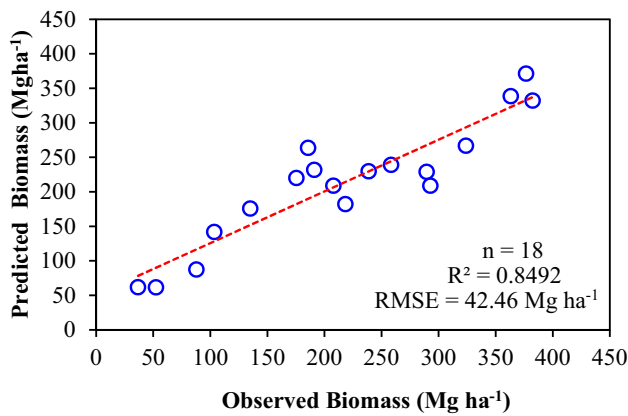


Fig. 6 Validation of field-observed versus RF-modeled AGB

deodara forest, *Quercus* mixed forest from 87.85 to 413.93 Mg ha⁻¹ (± 88.70 SD), mixed miscellaneous forest from 173.31 to 367.75 Mg ha⁻¹ (± 92.23 SD), in softwood *Pinus roxburghii* forest from 60.26 to 358.49 Mg ha⁻¹ (± 85.74 SD) and Scrub from 25.78 Mg ha⁻¹ to 46.27 Mg ha⁻¹ (± 12.98 SD). It may be discerned from the range of AGB that *Cedrus deodara* forests have good and uniform crop of tree and canopy density. Maximum range difference was noticed in

Quercus forest, which is an indication of site conditions and biotic pressures (*Quercus* is a chief fuel wood and fodder species). However, the vigor of the *Quercus* forest improves with slope at higher ridges. Inaccessibility to the area could be the possible reason for it. *Pinus roxburghii* forests grow on exposed, rocky, poor soil conditions having high biotic pressures, and hence varied range of AGB was observed. Lower AGB in *Pinus roxburghii* forest in comparison with *Quercus* mixed forest may be attributed to the high specific density of *Quercus* wood (Tiwari et al. 2005). The results are in close agreement with the study performed by Sharma et al. (2016) under similar forest types of the Garhwal Himalaya. AGB for *Quercus* mixed forest in this study was found lesser than Sharma et al. (2016); however, it was close to the AGB estimated by Dimri et al. (2017) under similar forest of Garhwal Himalaya.

For RF-based regression modeling of AGB, RFE ranked NDVI to be the most important predictor variable along with NNIR, ARVI, IPVI, GNDVI, etc., on the basis of %IncMSE and IncNode purity (Fig. 4). The individual spectral bands (B2, B3 and B4) also formed a robust combination for prediction of AGB (Kumar et al. 2011; Singh et al. 2012; Vicharnakorn et al. 2014) and the presence of textural variables improved the prediction accuracy

Table 2 Comparison of regression analysis-based models statistics for AGB prediction

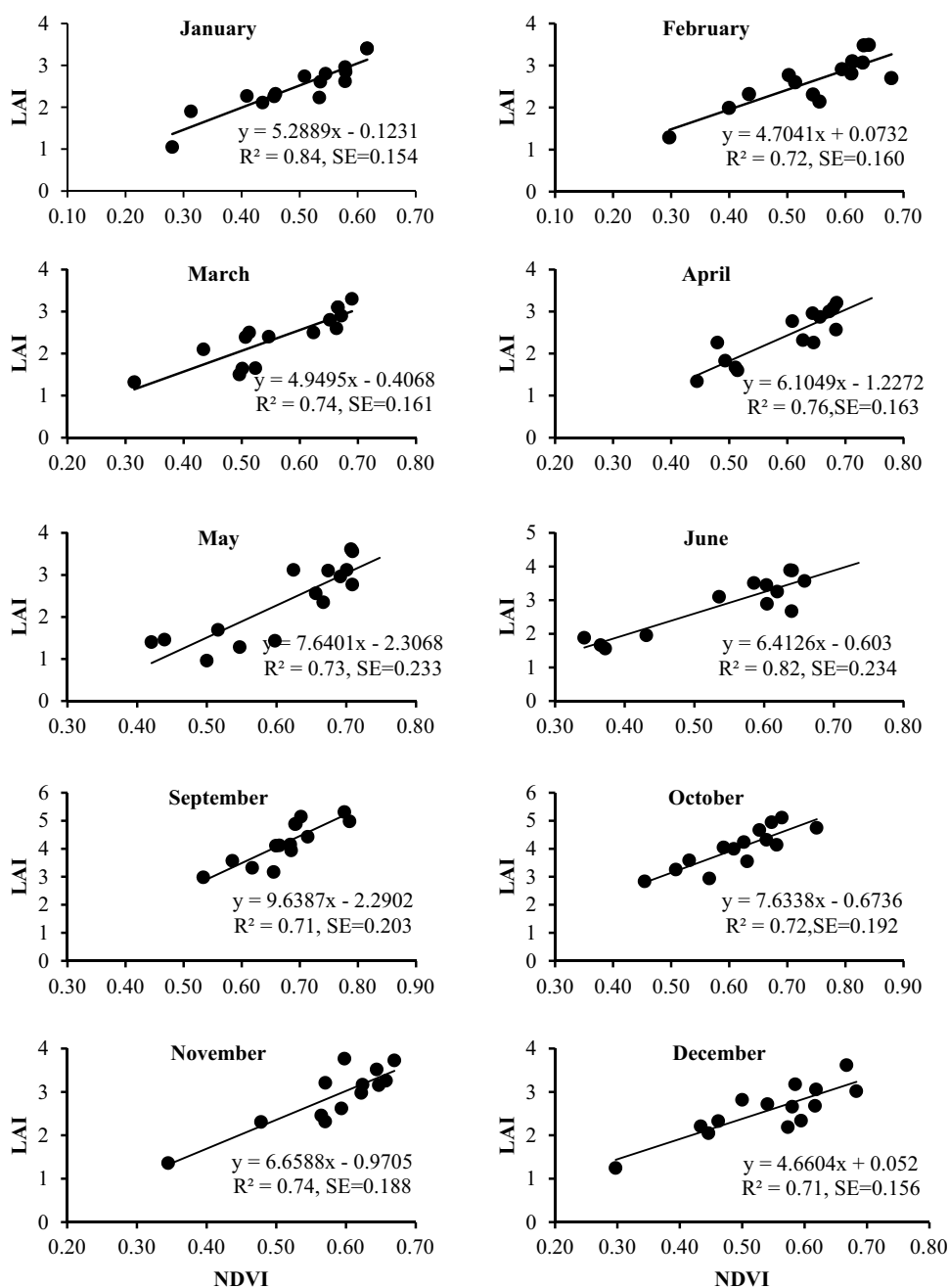
S. no.	Study area	Forest type	Satellite data	R ²	RMSE (Mg ha ⁻¹)	References
1.	KwaZulu-Natal Province, South Africa	Wetland vegetation	WorldView2	—	4.41	Mutanga et al. (2012)
2.	KwaZulu-Natal Province, South Africa	Eucalyptus species and Pine forest	Landsat 7,8 and ETM+	0.42, 0.32	55.32, 64.26	Dube and Mutanga (2015)
3.	Northern Daklak Province, Vietnam	Deciduous forest	Landsat8	0.48	46.22	Le et al. (2018)
4.	Daxing'anling Mountains in northeastern China	Mixed species	Landsat5/TM, GLAS	0.70	39.60	Liu et al. (2017)
5.	Parsa National Park, Nepal	Subtropical forest	Landsat8	0.95	13.3	Pandit et al. (2018b)
6.	Parsa National Park, Nepal	Subtropical forest	Sentinel2	0.81	25.57	Pandit et al. (2018a)
7.	Parsa National Park, Nepal	Subtropical forest	Sentinel2	0.99	4.51	Pandit et al. (2019)
8.	Katerniaghat Wildlife Sanctuary	Tropical forest	Sentinel1A	0.71, 0.60	105.03, 79.45	Ghosh and Behera (2018)
9.	Kashmir Valley, Western Himalaya, India	Temperate Forests (Broad leaved forest, <i>Abies pindrow</i> , <i>Pinus wallichiana</i> , and <i>Cedrus deodara</i>)	MODIS 250	0.85, 0.63, 0.58, and 0.42	38.60, 116.07, 119.24, and 85.27	Singh et al. (2012)
10.	Aglar watershed, Uttarakhand	<i>Pinus roxburghii</i> , <i>Cedrus deodara</i> , <i>Quercus</i> mixed, mixed forest	Landsat8	0.84	42.03	Present work

(Lu 2005). RF predicted highest AGB in *Cedrus deodara* forest ($407.73 \text{ Mg ha}^{-1}$) and minimum in mixed scrub (48.52 Mg ha^{-1}), in agreement with primary data. High AGB was in dense forests of *Quercus* mixed occurring on the higher ridges in the watershed (Fig. 5). However, the results indicated that RF underestimated in high-density forests with high AGB and overestimated in low-density forests with low AGB (Pandit et al. 2018a, b). The average value of modeled AGB was found to be $268.22 \text{ Mg ha}^{-1}$ in the present study. Singh et al. (2012) reported $210.48 \text{ Mg ha}^{-1}$ in temperate forest in north-western Himalaya in Kashmir valley. High AGB reported

in this study can be ascribed to favorable environmental conditions, viz. high moisture availability and soil organic carbon in Garhwal Himalaya as compared to dry temperate regions of Kashmir valley (Kishwan et al. 2009). pH plays important role in net carbon assimilation. The former has more acidic soils with pH ranging from 5.50 and 6.64, respectively (Gairola et al. 2012; Wani et al. 2014) which could also be a plausible reason behind it.

The validation of RF predicted vis-à-vis primary AGB at pixel-level gave coefficient of determination (R^2)=0.84, RMSE=42.46 Mg ha^{-1} , %RMSE=19.49%, MAPE and MAE equal to 19.94%, and 34.68 Mg ha^{-1} , respectively

Fig. 7 Scatter plot correlation analysis between filed-observed monthly LAI and NDVI



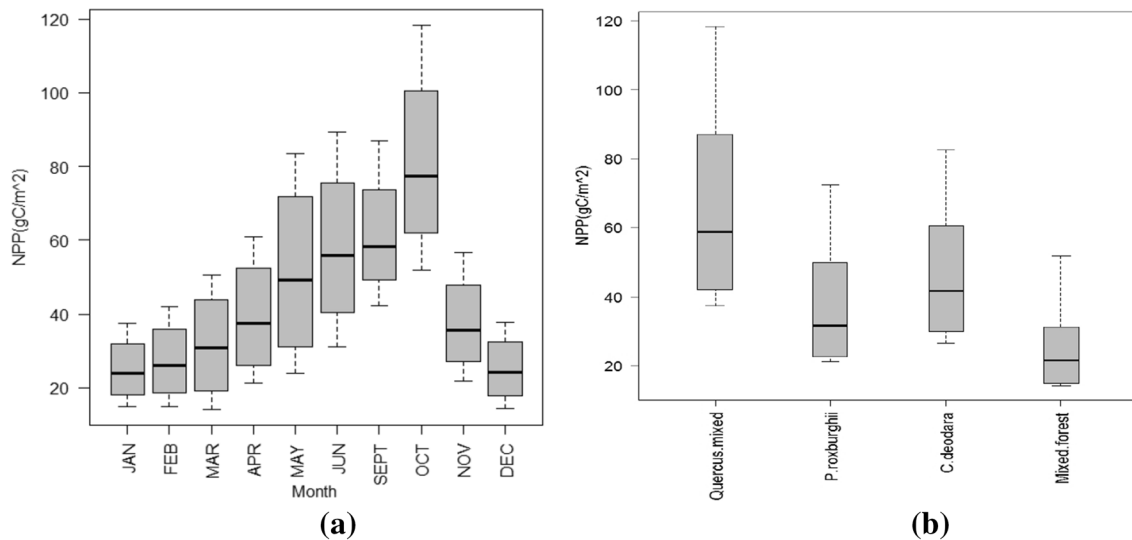


Fig. 8 Distribution of NPP statistics **a** overall monthly variation **b** forest-type-wise variation

Table 3 Comparison of NPP estimates among similar forest cover types in the world

S. no.	Study area	Forest cover types	Satellite data	Model used	Estimated NPP (gC/m ² /year)	References
1.	North America	Temperate forest	—	Osnabruck and Terrestrial Ecosystem Model	534.6–618.3	McGuire et al. (1993)
2.	North-Central Hampshire, USA	Temperate forest	AVIRIS	PnET-II	280–752	Ollinger and Smith (2005)
3.	South-East Paris	<i>Quercus</i> and <i>Pinus</i> species forest	SPOT	CASTANEA	672 and 658	Le Maire et al. (2005)
4.	China Province	^a BL, NL, mixed forest	Landsat TM and MODIS image	Boreal ecosystem productivity simulator	613.1, 456.8, 559.5	Feng et al. (2007)
5.	East Asia region located	^a BL, NL	AVHRR	CASA (LUE)	948.36, 369.66	Yu et al. (2009)
6.	Indian subcontinent	^a BL, NL	SPOT vegetation, METEOSAT-V, NOAA	CASA (LUE)	989, 557	Nayak et al. (2010)
7.	Indian subcontinent	^a BL	GIMMS, CRU-UEA, SPOT vegetation	CASA (LUE)	1057	Nayak et al. (2013)
8.	Aglar watershed, Uttarakhand	<i>Quercus</i> mixed, <i>Pinus roxburghii</i> and <i>Cedrus deodara</i> , mixed forest	Landsat-8 OLI	LUE	663.19, 468.79, 369.07 and 250.57	Present work

^aBL Broad leaf, NL Needle leaf

(Fig. 6). Safari et al. (2017) reported that RF outperforms with most important variables from Landsat-8 OLI data with low RMSE and moderate R^2 values. Table 2 compares model statistics obtained from various regression models used to assess AGB over the world.

Spatiotemporal pattern of NPP

Regression analysis performed between field-observed LAI vis-à-vis NDVI showed high correlation for each corresponding month (Fig. 7). Thus, NDVI images were used for

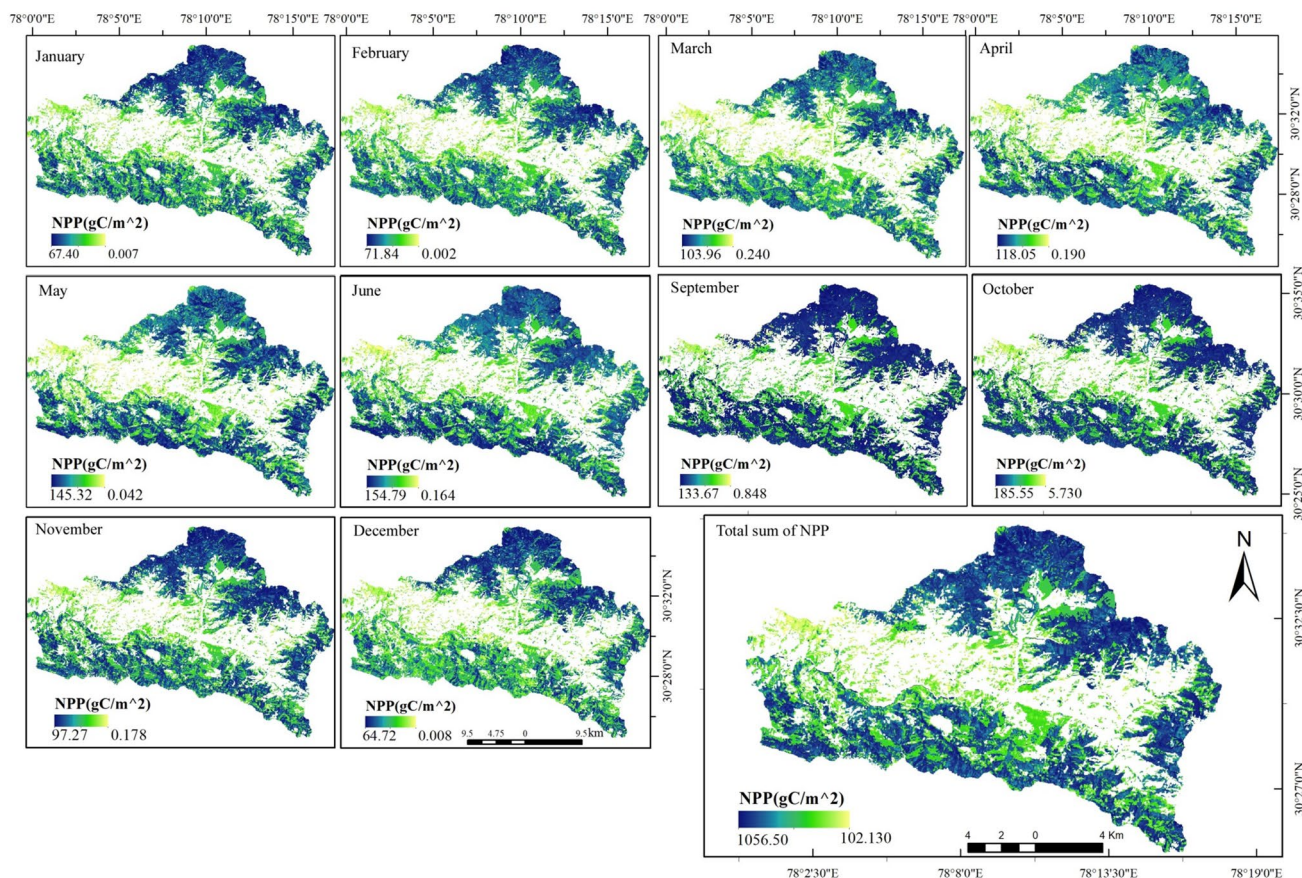


Fig. 9 Spatiotemporal distribution of NPP in Aglar watershed

geospatial modeling of LAI and fAPAR for each month. The NPP ranged from 102 to 1056 gC/m²/year with an average of 561.32 gC/m²/year. It was the highest in *Quercus* mixed forest (663.19 gC/m²/year) followed by forests of *Cedrus deodara*, *Pinus roxburghii* and mixed forest as 468.79, 369.07 and 250.57 gC/m²/year, respectively. Monthly variation of NPP among all the forest types studied is shown in Fig. 8a, b. Highest carbon assimilation of 95,148,073.9 gC/year has been found in *Quercus* mixed with evergreen broadleaf species, followed by needle-shaped leaf forest of *Cedrus deodara* and *Pinus roxburghii* as 5,752,954.1 gC/year and 1,863,187.7 gC/year and mixed forests 2,634,737.1 gC/year. A comparison of our findings with global reports is presented in Table 3.

Spatiotemporal variations in monthly NPP were noticed across the watershed (Fig. 9). The significant effect of climatic conditions, viz. temperature, precipitation events and PAR, was evident on forest productivity (Fig. 10). NPP peaked during growing season which starts from May and culminates in November–December (Fig. 10a). It was the highest in October which may be attributed to optimal

environmental conditions for photosynthesis soon after the receding of monsoon (Fig. 10b, c). The productivity begins to decline with the onset of dry winter months, i.e., December to January and the decrease in productivity continues till January. It is primarily due to very low temperature that decreases the rate of photosynthetic phenomenon (Zhu et al. 2006). With the rise in temperature and moisture condition in February, the leaf flushing or ‘green wave’ accelerates and this coupled with rise in temperature in the subsequent months helps in leaf expansion and maturity (Raich et al. 2006). However, at this stage dry summer alleviates the process of carbon assimilation by the plant foliage due to lack of moisture in soil and atmosphere. Such temporal variations of NPP were also reported by Feng et al. (2007) while studying temperate forests of China in the neighboring region. Other factors such as increased cloud cover reduces the availability of PAR (Beer et al. 2010) which negatively affects the process of carbon assimilation. This phenomenon was evident in the month of September (Fig. 10d). The NPP estimates for major forest types in this study were found coherent with the findings of Feng et al. (2007).

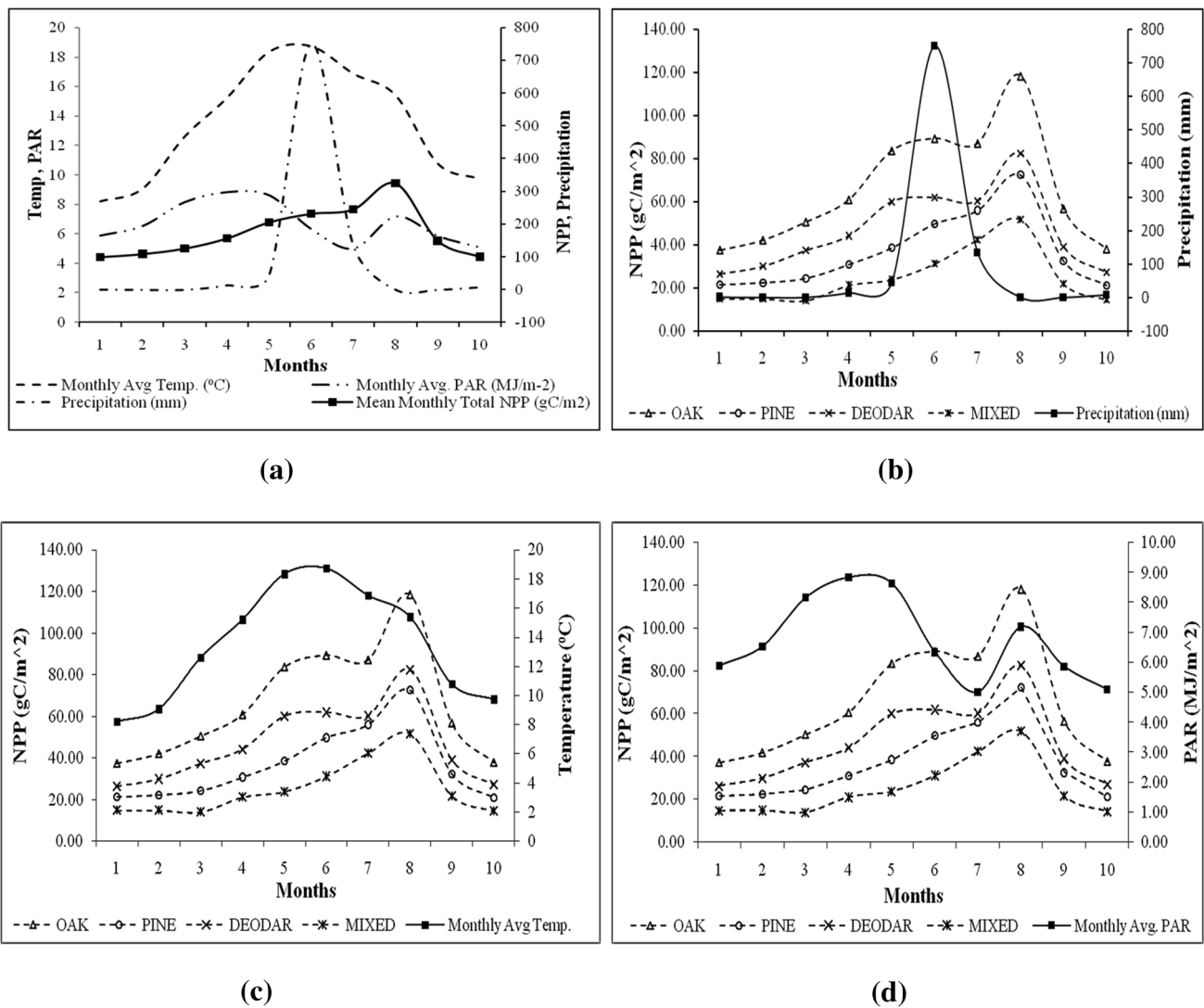


Fig. 10 Mean monthly variation in NPP w.r.t. a environmental variables and b, c, d are their effect on different forest types of Aglar watershed

Conclusion

Himalayan ecosystems exhibit intricate relationships among the environmental variables because of its arc-shape and complex terrain (slope, aspect, elevation) and varied orography. Forest biomass and NPP are recognized as important climate regulatory ecosystem services in South Asia furnished by Himalayan forest ecosystems. In-depth knowledge of these biophysical variables is helpful in manifesting forest ecosystems status/functioning, sequestration potential and for framing climate-change mitigation strategy. It is established from study that temporal primary data and corresponding seasonal earth observation data have good potential to estimate AGB using RF and NPP using LUE for geospatial modeling in a medium sized watershed. RF-based RFE function helped us in prioritizing and identifying the 24 most important variables out of 96 contributing to

AGB prediction. The results had low RMSE with high R^2 than other regression equation-based simple spectral models. The process-based models coupled with earth observation data provided better understanding of highly dynamic productivity in ecosystems. LUE is a most important factor for NPP assessment and is affected by climatic factors such as rainfall, temperature, moisture/humidity, PAR, age of the leaves and plant itself. However, PAR, temperature and precipitation were the dominant factors governing it. Climatically, Aglar watershed lies in the western most limits of humid temperate forests in outer Himalayan zone and not far from vast Indo-Gangetic Plains; thus, it is very likely that NPP would vary from other temperate regions with high or low rainfall and humidity. We report lesser NPP cf. with earlier reports from other temperate forest ecosystems. The approach is very robust and simple and can serve as a good alternative for reliable estimation of AGB and

carbon storage potential especially in areas where ground data is scarce. Such watershed-level study would help to understand complex biogeochemical processes by improving regional and global scale models of climate change and NPP. However, the NPP estimates need to be further tested and validated with in situ measurements, viz. carbon flux tower.

Acknowledgements Authors are grateful to Dr. Prakash Chauhan Director, Indian Institute of Remote Sensing, ISRO, for time to time encouragements and facilities. We thank Dr. Hitendra Padalia Head, Forestry & Ecology Department Indian Institute of Remote Sensing for his cooperation and administrative support. We are thankful to Dr. S. P. Aggarwal Head Water Resource Department and Dr. Praveen Thakur Senior Scientist Water Resource Department, IIRS, for maintaining AWS and providing meteorological data. We are also thankful to the authorities of Forest department of Uttarakhand, more specially to Chief Conservator of Forest, Uttarakhand, and Divisional Forest Officer of Mussoorie Forest Division for allowing us to conduct this study. We thank Range officers of the concerned ranges for their extended cooperation while collecting the field data. Srishti Gwal is also thankful to University Grant Commission for providing funds for this project. We are thankful to the anonymous reviewers for their valuable comments which have enhanced the worth of the work.

Author's contributions Srishti Gwal has performed data compilation, simulation, analysis and has drafted the manuscript. Sarnam Singh and Stutee Gupta contributed in reviewing and editing the manuscript. Shikha Anand supported during field data accumulation of this project.

Funding The present work is funded by University Grant Commission, Government of India (Grant No. 21/12/2014(ii)EU-V).

Availability of data and materials It is a Ph.D. research work. The data can be shared with terms and conditions with persons with valid research interests for verification and validation.

Compliance with ethical standards

Conflict of interest The authors declare that they have no conflict of interest.

References

- Bannari A, Morin D, Bonn F, Huete AR (1995) A review of vegetation indices. *Remote Sens Rev* 13:95–120. <https://doi.org/10.1080/02757259509532298>
- Bannari A, Asalhi H, Teillet PM (2002) Transformed difference vegetation index (TDVI) for vegetation cover mapping. *Int Geosci Remote Sens Symp* 5:3053–3055. <https://doi.org/10.1109/igars.2002.1026867>
- Bear C, Reichstein M, Tomelleri E et al (2010) Terrestrial gross carbon dioxide uptake: Global distribution and covariation with climate. *Science* 80(329):834–838. <https://doi.org/10.1126/science.1184984>
- Behera SK, Tripathi P, Behera MD, Tuli R (2019) Modeling net primary productivity of tropical deciduous forests in North India using bio-geochemical model. *Biodivers Conserv* 28:2105–2121. <https://doi.org/10.1007/s10531-019-01743-6>
- Belgiu M, Drăgu L (2016) Random forest in remote sensing: A review of applications and future directions. *ISPRS J Photogramm Remote Sens* 114:24–31. <https://doi.org/10.1016/j.isprsjprs.2016.01.011>
- Birth GS, McVey GR (1968) Measuring the color of growing turf with a reflectance spectrophotometer. *Agron J* 60:640–643. <https://doi.org/10.2134/agronj1968.00021962006000060016x>
- Breiman L (2001) Random forests. *Mach Learn* 45(1):5–32. <https://doi.org/10.1023/A:1010933404324>
- Chacko VJ (1965) A manual on sampling techniques for forest surveys. The Manager of Publications, Delhi, p 172
- Chave J, Olivier J, Bongers F, Chatelet P, Forget PM, Meer PVD, Norden N, Riera B, Charles-Dominique P (2008) Above-ground biomass and productivity in a rain forest of eastern South America. *J Trop Ecol* 24:355–366. <https://doi.org/10.1017/S0266467408005075>
- Chen JM (1996) Evaluation of vegetation indices and a modified simple ratio for boreal applications. *Can J Remote Sens* 22:229–242. <https://doi.org/10.1080/07038992.1996.10855178>
- Chhabra A, Dadhwal VK (2004) Estimating terrestrial net primary productivity over India using satellite data. *Curr Sci* 86:269–271
- Chitale VS, Tripathi P, Behera MD, Behera SK, Tuli R (2012) On the relationships among diversity, productivity and climate from an Indian tropical ecosystem: a preliminary investigation. *Biodivers Conserv* 21:1177–1197. <https://doi.org/10.1007/s10531-012-0247-9>
- Cramer W, Kicklighter DW, Bondeau A et al (1999) Comparing global models of terrestrial net primary productivity (NPP): overview and key results. *Glob Change Biol* 5:1–15. <https://doi.org/10.1046/j.1365-2486.1999.00009.x>
- Crippen RE (1990) Calculating the vegetation index faster. *Remote Sens Environ* 34:71–73. [https://doi.org/10.1016/0034-4257\(90\)90085-Z](https://doi.org/10.1016/0034-4257(90)90085-Z)
- Cunningham SC, Read J (2002) Comparison of temperate and tropical rainforest tree species: photosynthetic responses to growth temperature. *Oecologia* 133:112–119. <https://doi.org/10.1007/s00442-002-1034-1>
- Dadhwal VK (2012) Assessment of Indian carbon cycle components using earth observation systems and ground inventory. *ISPRS Int Arch Photogramm Remote Sens Spat Inf Sci XXXIX-B8:249–254*. <https://doi.org/10.5194/isprarchives-xxxix-b8-249-2012>
- Dang ATN, Nandy S, Srinet R, Luong NV, Ghosh S (2019) Forest aboveground biomass estimation using machine learning regression algorithm in Yok Don National Park, Vietnam. *Ecol Inform* 50:24–32. <https://doi.org/10.1016/j.ecoinf.2018.12.010>
- De Gier A (2003) A new approach to woody biomass assessment in woodlands and shrublands. In: Roy P (ed) *Geoinformatics for tropical ecosystems*, pp 161–198, India
- Deb Burman PK, Sarma D, Williams M, Karipot A, Chakraborty S (2017) Estimating gross primary productivity of a tropical forest ecosystem over north-east India using LAI and meteorological variables. *J Earth Syst Sci* 126:1–16. <https://doi.org/10.1007/s12040-017-0874-3>
- Devagiri GM, Money S, Singh S, Dadhwal VK, Patil P, Khaple A, Devakumar AS, Hubballi S (2013) Assessment of above ground biomass and carbon pool in different vegetation types of south western part of Karnataka, India using spectral modeling. *Trop Ecol* 54(2):149–165
- Dimri S, Baluni P, Sharma CM (2017) Biomass production and carbon storage potential of selected old-growth temperate forests in Garhwal Himalaya, India. *Proc Natl Acad Sci India Sect B Biol Sci* 87:1327–1333. <https://doi.org/10.1007/s40011-016-0708-0>
- Dixon RK, Brown S, Houghton RA, Solomon AM, Trexler MC, Wisniewski J (1994) Carbon pools and flux of dynamic forest ecosystems. *Science* 80(263):185–191. <https://doi.org/10.1126/science.263.5144.185>

- Dube T, Mutanga O (2015) Evaluating the utility of the medium-spatial resolution Landsat 8 multispectral sensor in quantifying above-ground biomass in Umgeni catchment, South Africa. *ISPRS J Photogramm Remote Sens* 101:36–46. <https://doi.org/10.1016/j.isprsjprs.2014.11.001>
- Feng X, Liu G, Chen JM, Chen M, Liu J, Ju WM, Sun R, Zhou W (2007) Net primary productivity of China's terrestrial ecosystems from a process model driven by remote sensing. *J Environ Manage* 85:563–573. <https://doi.org/10.1016/j.jenvman.2006.09.021>
- FRI (2002) Indian woods: their identification, properties and uses, vol I–VI (Revised edition). Forest Research Institute, Indian Council of Forestry Research and Education, Ministry of Environment and Forests, Government of India, Dehradun
- Friend AD, Cox PM (1995) Modelling the effects of atmospheric CO₂ on vegetation atmosphere interactions. *Agric For Meteorol* 73:285–295. [https://doi.org/10.1016/0168-1923\(94\)05079-L](https://doi.org/10.1016/0168-1923(94)05079-L)
- FSI (1996) Volume equations for forests of India Nepal and Bhutan. Forest Survey of India, Ministry of Environment and Forests, Govt. of India, pp 67,113,138,147, 150,156,202
- Gairola S, Sharma CM, Ghildiyal SK, Suyal S (2012) Chemical properties of soils in relation to forest composition in moist temperate valley slopes of Garhwal Himalaya, India. *Environmentalist* 32:512–523. <https://doi.org/10.1007/s10669-012-9420-7>
- Gamon JA, Surfus JS (1999) Assessing leaf pigment content and activity with a reflectometer. *New Phytol* 143:105–117. <https://doi.org/10.1046/j.1469-8137.1999.00424.x>
- Gao BC (1996) NDWI a normalized difference water index for remote sensing of vegetation liquid water from space. *Remote Sens Environ* 72:257–266. [https://doi.org/10.1016/s0034-4257\(96\)00067-3](https://doi.org/10.1016/s0034-4257(96)00067-3)
- Gasparri NI, Parmuchi MG, Bono J, Karszenbaum H, Montenegro CL (2010) Assessing multi-temporal Landsat 7 ETM+ images for estimating above-ground biomass in subtropical dry forests of Argentina. *J Arid Environ* 74:1262–1270. <https://doi.org/10.1016/j.jaridenv.2010.04.007>
- Ghosh SM, Behera MD (2018) Above ground biomass estimation using multi-sensor data synergy and machine learning algorithms in a dense tropical forest. *Appl Geogr* 96:29–40. <https://doi.org/10.1016/j.apgeog.2018.05.011>
- Gislason PO, Benediktsson JA, Sveinsson JR (2006) Random forests for land cover classification. *Pattern Recognit Lett* 27:294–300. <https://doi.org/10.1016/j.patrec.2005.08.011>
- Gitelson AA (2004) Wide dynamic range vegetation index for remote quantification of biophysical characteristics of vegetation. *J Plant Physiol* 161:165–173. <https://doi.org/10.1078/0176-1617-01176>
- Gitelson AA, Kaufman YJ, Merzlyak MN (1996) Use of a green channel in remote sensing of global vegetation from EOS-MODIS. *Remote Sens Environ* 58:289–298. [https://doi.org/10.1016/S0034-4257\(96\)00072-7](https://doi.org/10.1016/S0034-4257(96)00072-7)
- Gitelson AA, Stark R, Grits U, Rundquist D, Kaufman Y, Derry D (2002) Vegetation and soil lines in visible spectral space: a concept and technique for remote estimation of vegetation fraction. *Int J Remote Sens* 23:2537–2562. <https://doi.org/10.1080/01431160110107806>
- Goel NS, Qin W (1994) Influences of canopy architecture on relationships between various vegetation indices and LAI and FPAR: a computer simulation. *Remote Sens Rev* 10:309–347. <https://doi.org/10.1080/02757259409532252>
- Gong P, Pu R, Biging GS, Larrieu MR (2003) Estimation of forest leaf area index using vegetation indices derived from Hyperion hyperspectral data. *IEEE Trans Geosci Remote Sens* 41:1355–1362. <https://doi.org/10.1109/TGRS.2003.812910>
- Goroshi S, Singh RP, Pradhan R, Parihar JS (2014) Assessment of net primary productivity over India using Indian geostationary satellite (INSAT-3A) data. *Int Arch Photogramm Remote Sens Spat Inf Sci ISPRS Arch* 40(8):561–568. <https://doi.org/10.5194/isprsarchives-XL-8-561-2014>
- Guyon I, Elisseeff A (2003) An introduction to variable and feature selection isabelle. *J Mach Learn Res* 3:1157–1182
- Haralick RM (1979) Statistical and structural approaches to texture. *Proc IEEE* 67:786–804. <https://doi.org/10.1109/proc.1979.11328>
- Hardisky MA, Smart RM, Klemas V (1983) Seasonal spectral characteristics and aboveground biomass of the tidal marsh plant, *Spartina alterniflora*. *Am Soc Photogr* 49:77–83
- HariPriya GS (2002) Biomass carbon of truncated diameter classes in Indian forests. *For Ecol Manage* 168:1–13. [https://doi.org/10.1016/S0378-1127\(01\)00729-0](https://doi.org/10.1016/S0378-1127(01)00729-0)
- Haxeltine A, Prentice IC (1996) BIOME3: an equilibrium biosphere model based on ecophysiological constraints, resource availability and competition among plant functional types. *Glob Biogeochem Cycles* 10:693–709. <https://doi.org/10.1029/96GB02344>
- Huang N, Niu Z, Wu C et al (2010) Modeling net primary production of a fast-growing forest using a light use efficiency model. *Ecol Model* 221:2938–2948. <https://doi.org/10.1016/j.ecolmodel.2010.08.041>
- Huete AR (1988) A soil-adjusted vegetation index (SAVI). *Remote Sens Environ* 25:295–309. [https://doi.org/10.1016/0034-4257\(88\)90106-X](https://doi.org/10.1016/0034-4257(88)90106-X)
- India Meteorological Department (IMD) (2015) Ministry of Earth Sciences (MoES), Government of India, New Delhi. <http://www.imd.gov.in>
- Ismail R, Mutanga O (2010) A comparison of regression tree ensembles: predicting *Sirex noctilio* induced water stress in *Pinus patula* forests of KwaZulu-Natal South Africa. *Int J Appl Earth Obs Geoinf*. <https://doi.org/10.1016/j.jag.2009.09.004>
- Jarvis PG, Leverenz JW (1983) Productivity of temperate, deciduous and evergreen forests. *Physiol Plant Ecol IV*. https://doi.org/10.1007/978-3-642-68156-1_9
- Jurgens C (1997) The modified normalized difference vegetation index (mNDVI) a new index to determine frost damages in agriculture based on Landsat TM data. *Int J Remote Sens* 18:3583–3594. <https://doi.org/10.1080/014311697216810>
- Kale MP, Roy PS (2012) Net primary productivity estimation and its relationship with tree diversity for tropical dry deciduous forests of central India. *Biodivers Conserv* 21:1199–1214. <https://doi.org/10.1007/s10531-012-0226-1>
- Kale MP, Singh S, Roy PS (2002) Biomass and productivity estimation using aerospace data and geographic information system. *Trop Ecol* 43:123–136
- Kale M, Singh S, Roy PS (2005) Estimation of Leaf Area Index in dry deciduous forests from IRS-WiFS in central India. *Int J Remote Sens* 26:4855–4867. <https://doi.org/10.1080/01431160500181309>
- Kasischke ES, Goetz S, Hansen MC et al (2014) Remote sensing for natural resource management and environmental monitoring, 3rd edn. Wiley, New York
- Kaufman YJ, Tanre D (1992) Atmospherically Resistant Vegetation Index (ARVI) for EOS-MODIS. *IEEE Trans Geosci Remote Sens* 30:261–270. <https://doi.org/10.1109/36.134076>
- Kauth RJ (1976) Tasseled cap—a graphic description of the spectral-temporal development of agricultural crops as seen by Landsat, pp 41–51. http://docs.lib.purdue.edu/lars_symp/159
- Keeling HC, Phillips OL (2007) The global relationship between forest productivity and biomass. *Glob Ecol Biogeogr* 16:618–631. <https://doi.org/10.1111/j.1466-8238.2007.00314.x>
- Kender JR (1976) Saturation, hue, and normalized color: calculation, digitization effects, and use
- Kimura R, Okada S, Miura H, Kamichika M (2004) Relationships among the leaf area index, moisture availability, and spectral

- reflectance in an upland rice field. *Agric Water Manag* 69:83–100. <https://doi.org/10.1016/j.agwat.2004.04.009>
- Kishwan J, Pandey R, Dadhwal VK (2009) India's forest and tree cover: contribution as a carbon sink. *Tech Pap* 248006, pp 1–16
- Knapp AK, Smith MD (2001) Variation among biomes in temporal dynamics of aboveground primary production. *Science* 80(291):481–484. <https://doi.org/10.1126/science.291.5503.481>
- Kumar M, Monteith JL (1981) Remote sensing of crop growth. In: Smith H (ed) *Plants and daylight spectrum*. Academic Press, New York, pp 133–144
- Kumar R, Gupta SR, Singh S, Patil P, Dadhwal VK (2011) Spatial distribution of forest biomass using remote sensing and regression models in Northern Haryana, India. *Int J Ecol Environ Sci* 37:37–47
- Laurance WF, Fearnside PM, Laurance SG et al (1999) Relationship between soils and Amazon forest biomass: a landscape-scale study. *For Ecol Manage* 118:127–138. [https://doi.org/10.1016/S0378-1127\(98\)00494-0](https://doi.org/10.1016/S0378-1127(98)00494-0)
- Lawrence RL, Wood SD, Sheley RL (2006) Mapping invasive plants using hyperspectral imagery and Breiman Cutler classifications (randomForest). *Remote Sens Environ* 100:356–362. <https://doi.org/10.1016/j.rse.2005.10.014>
- Le Maire G, Davi H, Soudani K, Francois C, Le Dantec V, Dufrene E (2005) Modeling annual production and carbon fluxes of a large managed temperate forest using forest inventories, satellite data and field measurements. *Tree Physiol* 25:859–872. <https://doi.org/10.1093/treephys/25.7.859>
- Le AV, Paul DJ, Griffin AL (2018) Exploring the inclusion of small regenerating trees to improve above-ground forest biomass estimation using geospatial data. *Remote Sens* 10:1–27. <https://doi.org/10.3390/rs10091446>
- Lieth H (1975) Primary productivity of the biosphere. In: Lieth H, Whittaker RH (eds) *Primary productivity of the biosphere*. Springer, Berlin, pp 237–263. https://doi.org/10.1007/978-3-642-80913-2_12
- Liu K, Wang J, Zeng W, Song J (2017) Comparison and evaluation of three methods for estimating forest above ground biomass using TM and GLAS data. *Remote Sens* 9:341. <https://doi.org/10.3390/rs9040341>
- Lu D (2005) Aboveground biomass estimation using Landsat TM data in the Brazilian Amazon. *Int J Remote Sens* 26:2509–2525. <https://doi.org/10.1080/01431160500142145>
- Lu D (2006) The potential and challenge of remote sensing-based biomass estimation. *Int J Remote Sens* 27:1297–1328. <https://doi.org/10.1080/01431160500486732>
- Lu D, Mausel P, Brondizio E, Moran E (2004) Relationships between forest stand parameters and Landsat TM spectral responses in the Brazilian Amazon Basin. *For Ecol Manage* 198:149–167. <https://doi.org/10.1016/j.foreco.2004.03.048>
- Lu D, Xu X, Tian H, Moran E, Zhao M, Running S (2010) The effects of urbanization on net primary productivity in south-eastern China. *Environ Manage* 46:404–410. <https://doi.org/10.1007/s00267-010-9542-y>
- Lymburner L, Beggs PJ, Jacobson CR (2000) Estimation of canopy-average surface-specific leaf area using Landsat TM data. *Photogramm Eng Remote Sens* 66:183–191
- Maisongrand P, Ruimy A, Dedieu G, Saugier B (1995) Monitoring seasonal and interannual variations of gross primary productivity, net primary productivity and net ecosystem productivity using a diagnostic model and remotely-sensed data. *Tellus B Chem Phys Meteorol* 47(1–2):178–190. <https://doi.org/10.3402/tellusb.v47i1-2.16039>
- Majasalmi T, Rautiainen M (2016) The potential of Sentinel-2 data for estimating biophysical variables in a boreal forest: a simulation study. *Remote Sens Lett* 7(5):427–436. <https://doi.org/10.1080/2150704X.2016.1149251>
- Malhi Y, Baker TR, Phillips OL et al (2004) The above-ground coarse wood productivity of 104 neotropical forest plots. *Glob Change Biol* 10:563–591. <https://doi.org/10.1111/j.1529-8817.2003.00778.x>
- Manna S, Nandy S, Chanda A, Akhand A, Hazra S, Dadhwal VK (2014) Estimating aboveground biomass in *Avicennia marina* plantation in Indian Sundarbans using high-resolution satellite data. *J Appl Remote Sens* 8:083638. <https://doi.org/10.1117/1.jrs.8.083638>
- McGuire AD, Joyce LA, Kicklighter DW, Melillo JM, Esser G, Vorosmarty CJ (1993) Productivity response of climax temperate forests to elevated temperature and carbon dioxide: a North American comparison between two global models. *Clim Change* 24:287–310. <https://doi.org/10.1007/BF01091852>
- Meacham M, Queiroz C, Peterson GD (2016) Social-ecological drivers of multiple ecosystem services: What variables explain patterns of ecosystem services across the Norrström drainage basin? *Ecol Soc*. <https://doi.org/10.5751/ES-08077-210114>
- Melillo JM, McGuire AD, Kicklighter DW, Moore B III, Vorosmarty CJ, Schloss AL (1993) Global climate change and terrestrial net primary production. *Nature* 363:234–240. <https://doi.org/10.1038/363234a0>
- Monteith JL (1972) Solar radiation and productivity in tropical ecosystems. *J Appl Ecol* 9:747. <https://doi.org/10.2307/2401901>
- Mutanga O, Adam E, Cho MA (2012) High density biomass estimation for wetland vegetation using worldview-2 imagery and random forest regression algorithm. *Int J Appl Earth Obs Geoinf* 18:399–406. <https://doi.org/10.1016/j.jag.2012.03.012>
- Myneni RB, Hall FG, Sellers PJ, Marshak AL (1995) Interpretation of spectral vegetation indexes. *IEEE Trans Geosci Remote Sens* 33:481–486. <https://doi.org/10.1109/36.377948>
- Nayak RK, Patel NR, Dadhwal VK (2010) Estimation and analysis of terrestrial net primary productivity over India by remote-sensing-driven terrestrial biosphere model. *Environ Monit Assess* 170:195–213. <https://doi.org/10.1007/s10661-009-1226-9>
- Nayak RK, Patel NR, Dadhwal VK (2013) Inter-annual variability and climate control of terrestrial net primary productivity over India. *Int J Climatol* 33:132–142. <https://doi.org/10.1002/joc.3414>
- Nayak RK, Patel NR, Dadhwal VK (2015) Spatio-temporal variability of net ecosystem productivity over India and its relationship to climatic variables. *Environ Earth Sci* 74:1743–1753. <https://doi.org/10.1007/s12665-015-4182-4>
- Nelson RF, Kimes DS, Salas WA, Routhier M (2000) Secondary forest age and tropical forest biomass estimation using thematic mapper imagery. *Biogeosciences* 50:419–431. [https://doi.org/10.1641/0006-3568\(2000\)050%5b0419:SFAATF%5d2.0.CO;2](https://doi.org/10.1641/0006-3568(2000)050%5b0419:SFAATF%5d2.0.CO;2)
- Nemani RR, Keeling CD, Hashimoto H, Jolly WM, Piper SC, Tucker CJ, Myneni RB, Running SW (2003) Climate-driven increases in global terrestrial net primary production from 1982 to 1999. *Science* 80(300):1560–1563. <https://doi.org/10.1126/science.1082750>
- Ollinger SV, Smith ML (2005) Net primary production and canopy nitrogen in a temperate forest landscape: an analysis using imaging spectroscopy, modeling and field data. *Ecosystems* 8:760–778. <https://doi.org/10.1007/s10021-005-0079-5>
- Pan Y, Richard A, Pekka E et al (2011) A large and persistent carbon sink in the world's forests. *Science* 80(333):988–993. <https://doi.org/10.1126/science.1201609>
- Pandit S, Tsuyuki S, Dube T (2018a) Estimating above-ground biomass in sub-tropical buffer zone community forests, Nepal, using Sentinel 2 data. *Remote Sens* 10(4):601. <https://doi.org/10.3390/rs10040601>
- Pandit S, Tsuyuki S, Dube T (2018b) Landscape-scale aboveground biomass estimation in buffer zone community forests of Central Nepal: coupling in situ measurements with Landsat 8 Satellite

- Data. *Remote Sens* 10(11):1848. <https://doi.org/10.3390/rs10111848>
- Pandit S, Tsuyuki S, Dube T (2019) Exploring the inclusion of Sentinel-2 MSI texture metrics in above-ground biomass estimation in the community forest of Nepal. *Geocarto Int.* <https://doi.org/10.1080/10106049.2019.1588390>
- Patenaude G, Milne R, Dawson TP (2005) Synthesis of remote sensing approaches for forest carbon estimation: reporting to the Kyoto Protocol. *Environ Sci Policy* 8:161–178. <https://doi.org/10.1016/j.envsci.2004.12.010>
- Potter CS, Randerson JT, Field CB, Matson PA, Vitousek PM, Mooney HA, Klooster SA (1993) Terrestrial ecosystem production: process model based on global satellite and surface data. *Global Biogeochem Cycles* 7:811–841. <https://doi.org/10.1029/93GB02725>
- Potter C, Klooster S, Myneni R, Genovese V, Tan PN, Kumar V (2003) Continental-scale comparisons of terrestrial carbon sinks estimated from satellite data and ecosystem modeling 1982–1998. *Glob Planet Change* 39:201–213. <https://doi.org/10.1016/j.gloplacha.2003.07.001>
- Prince SD, Goward SJ (1995) Global primary production: a remote sensing approach. *J Biogeogr* 22:316–336. <https://doi.org/10.2307/2845983>
- Qi J, Chehbouni A, Huete AR, Kerr YH, Sorooshian S (1994) A modify soil adjust vegetation index. *Remote Sens Environ* 48(2):119–126. [https://doi.org/10.1016/0034-4257\(94\)90134-1](https://doi.org/10.1016/0034-4257(94)90134-1)
- Raich JW (1991) Potential net primary productivity in South America: application of a global model. *Ecol Appl* 1:399–429. <https://doi.org/10.2307/1941899>
- Raich JW, Russell AE, Kitayama K, Patron WJ, Vitousek PM (2006) Temperature influences carbon accumulation in moist tropical forests. *Ecology* 87:76–87. <https://doi.org/10.1890/05-0023>
- Ravindranath NH, Ostwald M (2008) Carbon inventory methods handbook for greenhouse gas inventory, carbon mitigation and roundwood production projects. *Advances in global change research*. Springer, Berlin. <https://doi.org/10.1007/978-1-4020-6547-7>
- Raymond HE, Rock BN, Nobel PS (1987) Measurement of leaf relative water content by infrared reflectance. *Remote Sens Environ* 22:429–435. [https://doi.org/10.1016/0034-4257\(87\)90094-0](https://doi.org/10.1016/0034-4257(87)90094-0)
- Rondeaux G, Steven M, Baret F (1996) Optimization of soil-adjusted vegetation indices. *Remote Sens Environ* 55:95–107. [https://doi.org/10.1016/0034-4257\(95\)00186-7](https://doi.org/10.1016/0034-4257(95)00186-7)
- Rosillo-Calle F (2007) *The biomass assessment handbook*. Routledge Taylor and Francis, Abingdon. <https://doi.org/10.4324/9781849772884>
- Roujean JL, Breon FM (1995) Estimating PAR absorbed by vegetation from bidirectional reflectance measurements. *Remote Sens Environ* 51:375–384. [https://doi.org/10.1016/0034-4257\(94\)00114-3](https://doi.org/10.1016/0034-4257(94)00114-3)
- Rouse JW, Hass RH, Schell JA, Deering DW (1973) Monitoring vegetation systems in the great plains with ERTS. In: *Third earth resour technol satell symp*, vol 1, pp 309–317
- Roy PS, Jain A (1998) A satellite remote sensing based approach to estimate regional net primary productivity of forest. *Global change studies scientific results from ISRO geosphere biosphere program*
- Roy PS, Ravan SA (1996) Biomass estimation using satellite remote sensing data—an investigation on possible approaches for natural forest. *J Biosci* 21:535–561. <https://doi.org/10.1007/BF02703218>
- Ruimy A, Kergoat L, Bondeau A (1999) Comparing global models of terrestrial net primary productivity (NPP): analysis of differences in light absorption and light-use efficiency. *Glob Change Biol* 5:56–64. <https://doi.org/10.1046/j.1365-2486.1999.00007.x>
- Safari A, Sohrabi H, Powell S, Shataee S (2017) A comparative assessment of multi-temporal Landsat 8 and machine learning algorithms for estimating aboveground carbon stock in copice oak forests. *Int J Remote Sens* 38:6407–6432. <https://doi.org/10.1080/01431161.2017.1356488>
- Salunkhe O, Khare PK, Sahu TR, Singh S (2016) Estimation of tree biomass reserves in tropical deciduous forests of Central India by non-destructive approach. *Trop Ecol* 57(2):153–161
- Sharma CM, Mishra AK, Krishan R, Tiwari OP, Rana YS (2016) Variation in vegetation composition, biomass production, and carbon storage in ridge top forests of high mountains of Garhwal Himalaya. *J Sustain For* 35:119–132. <https://doi.org/10.1080/10549811.2015.1118387>
- Shirima DD, Pfeifer M, Platts PJ, Totland O, Moe SR (2015) Interactions between canopy structure and herbaceous biomass along environmental gradients in moist forest and dry miombo woodland of Tanzania. *PLoS ONE* 10:1–15. <https://doi.org/10.1371/journal.pone.0142784>
- Singh RP, Rovshan S, Goroshi SK, Panigrahy S, Parihar JS (2011) Spatial and temporal variability of net primary productivity (NPP) over terrestrial biosphere of India using NOAA-AVHRR based GloPEM model. *J Indian Soc Remote Sens* 39:345–353. <https://doi.org/10.1007/s12524-011-0123-1>
- Singh S, Dadhwal VK, Patil P (2012) Assessment of aboveground phytomass in temperate forests of Kashmir valley, J & K, India. *Int J Ecol Environ Sci* 38:47–58
- Singh N, Patel NR, Bhattacharya BK, Soni P, Parida BR, Parihar JS (2014) Analyzing the dynamics and inter-linkages of carbon and water fluxes in subtropical pine (*Pinus roxburghii*) ecosystem. *Agric For Meteorol* 197:206–218. <https://doi.org/10.1016/j.agrfor.2014.07.004>
- Sripada RP, Heiniger RW, White JG, Meijer AD (2006) Aerial color infrared photography for determining early in-season nitrogen requirements in corn. *Agron J* 98:968–977. <https://doi.org/10.2134/agronj2005.0200>
- Steininger MK (2000) Satellite estimation of tropical secondary forest above-ground biomass: data from Brazil and Bolivi. *Int J Remote Sens* 21:1139–1157. <https://doi.org/10.1080/014311600210119>
- Teluguntla P, Thenkabail P, Oliphant A, Xiong J, Gumma MK, Congalton RG, Yadav K, Huete A (2018) A 30-m Landsat-derived cropland extent product of Australia and China using random forest machine learning algorithm on Google Earth Engine cloud computing platform. *ISPRS J Photogramm Remote Sens* 144:325–340. <https://doi.org/10.1016/j.isprsjprs.2018.07.017>
- Tiwari AK (1994) Mapping forest biomass through digital processing of IRS-1A data. *Int J Remote Sens* 15:1849–1866. <https://doi.org/10.1080/01431169408954212>
- Tiwari AK, Singh JS (1984) Mapping forest biomass in India through aerial photographs and nondestructive field sampling. *Appl Geogr* 4:151–165. [https://doi.org/10.1016/0143-6228\(84\)90019-5](https://doi.org/10.1016/0143-6228(84)90019-5)
- Tiwari AK, Agarwal A, Kumar S, Tiwari SC (2005) Analysis of landuse and biomass in Khanda watershed, Garhwal Himalaya, using satellite remote sensing data. *Trop Ecol* 46:253–264
- Tripathi P, Patel NR, Kushwaha SPS (2018) Estimating net primary productivity in tropical forest plantations in India using satellite-driven ecosystem model. *Geocarto Int* 33:988–999. <https://doi.org/10.1080/10106049.2017.1323963>
- Tucker CJ (1979) Red and photographic infrared linear combinations for monitoring vegetation. *Remote Sens Environ* 8:127–150. [https://doi.org/10.1016/0034-4257\(79\)90013-0](https://doi.org/10.1016/0034-4257(79)90013-0)
- Uppgupta S, Singh S, Tiwari PS (2015) Estimation of aboveground phytomass of plantations using digital photogrammetry and high resolution remote sensing data. *J Indian Soc Remote Sens* 43:311–323. <https://doi.org/10.1007/s12524-014-0401-9>
- Vicharnakorn P, Shrestha RP, Nagai M et al (2014) Carbon stock assessment using remote sensing and forest inventory data in Savanna khet, Lao PDR. *Remote Sens* 6:5452–5479. <https://doi.org/10.3390/rs6065452>
- Vogelmann, J.E. and Rock BN (1985) Spectral characterization of suspected acid deposition damage in red spruce (*Picea rubens*)

- stands from Vermont. *Airborne Imaging Spectrometer Data Anal*, pp 51–55
- Wani AA, Joshi PK, Singh O, Bhat JA (2014) Estimating soil carbon storage and mitigation under temperate coniferous forests in the southern region of Kashmir Himalayas. *Mitig Adapt Strateg Glob Change* 19:1179–1194. <https://doi.org/10.1007/s11027-013-9466-y>
- Warnant P, FrancÈois L, Strivay D, Gerard JC (1994) CARAIB: a global model of terrestrial biological productivity. *Glob Biogeochem Cycles* 8:255–270. <https://doi.org/10.1029/94GB00850>
- Xiao X, Hollinger D, Aber J, Goltz M, Davidson EA, Zhang Q, Moore B III (2004) Satellite-based modeling of gross primary production in an evergreen needleleaf forest. *Remote Sens Environ* 89:519–534. <https://doi.org/10.1016/j.rse.2003.11.008>
- Xiao X, Zhang Q, Saleska S, Hutyrá L, Camargo PD, Wofsy S, Frohking S, Boles S, Keller M, Moore B III (2005) Satellite-based modeling of gross primary production in a seasonally moist tropical evergreen forest. *Remote Sens Environ* 94:105–122. <https://doi.org/10.1016/j.rse.2004.08.015>
- Yu D, Shi P, Shao H, Zhu W, Pan Y (2009) Modelling net primary productivity of terrestrial ecosystems in East Asia based on an improved CASA ecosystem model. *Int J Remote Sens* 30:4851–4866. <https://doi.org/10.1080/01431160802680552>
- Zanter K (2016) Landsat 8 (L8) Data Users Handbook. Dep Inter US GeolSurv NASA, vol 8, pp 97
- Zhu W, Pan Y, Liu X, Wang A (2006) Spatio-temporal distribution of net primary productivity along the northeast China transect and its response to climatic change. *J For Res* 17:93–98. <https://doi.org/10.1007/s11676-006-0022-4>

Publisher's Note Springer Nature remains neutral with regard to jurisdictional claims in published maps and institutional affiliations.